TABLE I
OPTIMUM LPD FOR ECG SIGNAL PROCESSING AT SAMPLING RATES f_s = 200, 250, 300 Hz IN THE THREE CASES CONSIDERED IN TEXT. (NORMALIZATION FACTOR d VALUE CAN BE CALCULATED FROM EQUATIONS (11a, b) AND (5)

QRS Detection		$d(\overline{C}_1, \overline{C}_2, \overline{C}_3, \overline{C}_4)_{s,a}$		
		f_s = 200 Hz	f_s = 250 Hz	f_s = 300 Hz
	*QRS-D*1:	$1/1.5\ (0, 1, 0, 0)_a$	$1/2\ (0, 1, 0, 0)_s$	$1/2.5\ (0, 0, 1, 0)_a$
	*QRS-D*2:	$1/21.5\ (0, 6, 5, 0)_a$	$1/38.5\ (0, 9, 10, 0)_a$	$1/5\ (0, 1, 1, 0)_s$
	*QRS-D*3:	$1/43\ (8, 10, 5, 0)_s$	$1/37\ (4, 6, 7, 0)_s$	$1/82\ (0, 8, 10, 9)_a$
PT Detection				
		f_s = 200 Hz $d(\overline{C}_7, \overline{C}_8, \overline{C}_9, \overline{C}_{10})_{s,a}$	f_s = 250 Hz $d(\overline{C}_9, \overline{C}_{10}, \overline{C}_{11}, \overline{C}_{12})_{s,a}$	f_s = 300 Hz $d(\overline{C}_{11}, \overline{C}_{12}, \overline{C}_{13}, \overline{C}_{14})_{s,a}$
	*PT-D*1:	$1/8\ (0, 1, 0, 0)_s$	$1/11.5\ (0, 0, 0, 1)_a$	$1/12.5\ (0, 0, 1, 0)_a$
	*PT-D*2:	$1/16\ (0, 1, 1, 0)_a$	$1/21\ (0, 1, 1, 0)_s$	$1/24\ (0, 1, 1, 0)_s$
	*PT-D*3:	$1/24\ (1, 1, 1, 0)_s$	$1/31.5\ (0, 1, 1, 1)_a$	$1/37.5\ (0, 1, 1, 1)_a$
PT/QRS Enhancement			$d(\overline{C}_i, \overline{C}_j, \cdots)$	
		f_s = 200 Hz	f_s = 250 Hz	f_s = 300 Hz
	*PT-QRS*1:	$1/8.5\ (\overline{C}_9 = 1)_a$	$1/10.5\ (\overline{C}_{11} = 1)_a$	$1/13\ (\overline{C}_{13} = 1)_s$
	*PT-QRS*2:	$1/17\ (\overline{C}_7 = 1, \overline{C}_{11} = 1)_a$	$1/21\ (\overline{C}_9 = 1, \overline{C}_{13} = 1)_a$	$1/25\ (\overline{C}_{10} = 1, \overline{C}_{15} = 1)_s$
	*PT-QRS*3:	$1/24\ (\overline{C}_4 = 1, \overline{C}_8 = 1, \overline{C}_{12} = 1)_s$	$1/30\ (\overline{C}_5 = 1, \overline{C}_{10} = 1, \overline{C}_{15} = 1)_s$	$1/36\ (\overline{C}_6 = 1, \overline{C}_{12} = 1, \overline{C}_{18} = 1)_s$

neurophysiologic work where neural spike signals are recorded by microelectrodes and must be discriminated from the background noise of the brain. An LPD filter may be employed here to detect neural spikes in real time.

REFERENCES

[1] J. Pan and W. J. Tompkins, "A real-time *QRS* detection algorithm," *IEEE Trans. Biomed. Eng.*, vol. BME-32, pp. 230–236, Mar. 1985.

[2] O. Pahlm and L. Sornmo, "Software *QRS* detection in ambulatory monitoring—A review," *Med. Biol. Eng. Comput.*, vol. 22, pp. 289–297, 1984.

[3] U. Shiro and A. Itzhak, "Digital low-pass differentiation for biological signal processing," *IEEE Trans. Biomed. Eng.*, vol. BME-29, pp. 686–693, Oct. 1982.

[4] B. Andrews and D. Jones, "A note of the differentiation of human kinematic data," in *Dig. 11th Int. Conf. Med. Biol. Eng.*, Ottawa, Ont., Canada, 1976, pp. 88–89.

[5] M. D. Lesh, J. M. Mansour, and S. R. Simon, "A gait analysis subsystem for smoothing and differentiation of human motion data," *J. Biomed. Eng.*, vol. 101, pp. 203–212, 1979.

[6] N. V. Thakor, J. G. Webster, and W. J. Tompkins, "Estimation of *QRS* Complex Power Spectra for Design of a *QRS* Filter," *IEEE Trans. Biomed. Eng.*, vol. BME-31, pp. 702–706, Nov. 1984.

A Perfused Tissue Phantom for Ultrasound Hyperthermia

P. J. BENKESER, L. A. FRIZZELL, K. R. HOLMES, AND S. A. GOSS

***Abstract*—A perfused tissue phantom, developed as a tool for analyzing the performance of ultrasound hyperthermia applicators, was investigated. The phantom, consisting of a fixed porcine kidney with thermocouples placed throughout the tissue, was perfused with degassed water by a variable flow rate pump. The phantom was insonated by an unfocused multielement ultrasound applicator and the temperatures in the phantom were recorded. The results indicate that for testing protocols where tissue phantoms are needed, the fixed kidney preparation offers an opportunity to use a more realistic phantom than has previously been available to assess the heating performance of ultrasound hyperthermia applicators.**

Manuscript received November 21, 1988; revised August 11, 1989. This work was supported in part by Labthermics Technologies, Inc., NIH Training Grant CA09067, and Grant NIH -HL27011.

P. J. Benkeser is with the School of Electrical Engineering, Georgia Institute of Technology, Atlanta, GA 30332.

L. A. Frizzell is with the Bioacoustics Research Laboratory, Department of Electrical and Computer Engineering, University of Illinois, Urbana, IL 61801.

K. R. Holmes is with the Department of Veterinary Bioscience and Bioengineering Faculty, University of Illinois, Urbana, IL 61801.

S. A. Goss is with Labthermics Technologies, Inc., Champaign, IL 61820.

IEEE Log Number 8933602.

I. INTRODUCTION

The goal of hyperthermic treatment of a tumor is to elevate the temperature of its entire volume to the therapeutic range, typically 43–45°C. Perfusion plays an important role in shaping the temperature distribution in tissues heated with hyperthermia applicators, and can vary significantly during the course of a given treatment [1]–[3]. To experimentally evaluate the performance of an applicator in a treatment simulation, a perfused tissue phantom must be employed in order to obtain realistic temperature distributions.

Due to the complex blood perfusion patterns present in normal tissue and tumors, it is difficult to construct a phantom to simulate these patterns [4]. Several simple dynamic phantoms have been constructed for microwave hyperthermia purposes [5], [6]. The flow geometry through these phantoms is quite different from that in tissue. Because of this difference, the temperature distributions obtained with these phantoms possess a questionable relationship to actual patient temperatures [4]. The use of dog kidneys and thigh muscles as *in vivo* thermal models have been reported by several researchers [7], [8]. However, the experimental complexity associated with these *in vivo* models makes them impractical as a simple and repeatable system for assessing the heating capabilities of a particular applicator design.

The purpose of the present work is to determine if a recently developed perfused tissue phantom can serve as a simple and easy to maintain device for analyzing more realistically the heating capabilities of ultrasound hyperthermia applicators.

II. METHODS AND MATERIALS

A. Perfused Tissue Phantom

The perfused tissue phantom employed in this study was an alcohol-fixed porcine kidney. This preparation possesses a system of perfusion channels whose structure closely resembles that of the

living organ. The anatomy of the kidney is very similar to the anatomy of many, if not most, solid tumors [9] in that the peripherally located cortex with its high tissue perfusion resembles the vascularized periphery of a tumor while the centrally-located medulla, with its very low tissue perfusion, approximates the lack of perfusion in the necrotic core of the tumor. The alcohol fixation technique has been reported previously [10].

The fixed kidney phantoms have been successfully preserved for more than two years. If proper care is taken to ensure that the perfusate is free of bubbles (degassed) and debris (filtering with a 5 μm pore filter size), the kidney can be repeatedly cycled through the fixation process for storage and the rehydration process for the phantom studies. It is not uncommon for a kidney to go through both of these processes more than ten times.

In studies of the H_2O content of freshly excised and ROH fixed rabbit kidneys, it was shown that the H_2O content of the fresh medulla was approximately 7% higher than that of the cortex [11]. However, in the rehydrated fixed kidney, which contained nearly 10% more H_2O than the fresh kidney, the percent H_2O content of the cortex and medulla were essentially equivalent [10]. It is speculated that the ROH dissolves, or permits the washout of some fraction of tissue lipids to the water of rehydration, and thus increases the H_2O content of the cortex.

The fixation process is estimated to increase the H_2O content from 77.8% in the freshly excised pig kidney [12] to approximately 85% for the rehydrated fixed kidney. This estimate of the H_2O content of the fixed kidney enables its specific heat c_m to be estimated from the following relationship [13]

$$c_m = 41.9\left[\%H_2O + 0.4(100 - \%H_2O)\right] J \cdot kg^{-1} \cdot K^{-1}. \quad (1)$$

Therefore, the c_m of the fixed kidney is approximately 3800 J $\cdot$ $kg^{-1} \cdot K^{-1}$. This value was used for all thermal washout calculations.

The fixed kidney phantom was mounted in a Plexiglass frame and placed in a tank filled with degassed water at 23°C. A calibrated, variable flow rate roller pump was connected to the renal artery of the kidney and circulated the degassed water perfusate which was drawn from the tank. Perfusate leaving the kidney via the renal vein was allowed to drain directly into the tank. The pump is capable of producing flow rates similar to those found in human tumors, which generally range from 0.2 to 17.0 kg $\cdot$ $m^{-3} \cdot s^{-1}$ [14]. This experimental setup is shown in Fig. 1.

The absorption coefficient in the freshly excised and ROH fixed kidney was measured using the transient thermoelectric technique [15], [16]. The purpose of these measurements was not only to determine the effect that the fixation process had on the absorption coefficient, but also to permit quantitative measurements of the intensity within the phantom.

B. Temperature Measurements

Temperatures in the phantom were measured using as many as 16 lap-soldered copper-constantan bare-wire thermocouples (75 μm wire size) inserted at various depths and lateral positions. The thermocouples can be removed and repositioned in the phantom if necessary. The temperatures were measured, with an accuracy of 0.1°C, by a 16-channel thermometry system (Labthermics Technologies, Inc. LT-100). The thermometry system transferred the temperature data acquired from all channels every 2 s to a microcomputer (Apple IIe) which stored all data on a floppy disk for later analysis.

To simplify the analysis of the thermal response of the phantom, the effects of conduction and perfusion were combined into a single "effective" perfusion term W_e [17]. This term was employed to analyze the thermal washout curve, which is the temperature versus time response when the applied power is removed from the phantom. This curve can be obtained from

$$T - T_w = (T_0 - T_w)e^{-(w_e c_w/\rho c_m)t} \quad (2)$$

where T_0 is the tissue temperature (°C) immediately preceeding the removal of the applied power; T and T_w are the tissue and perfusate

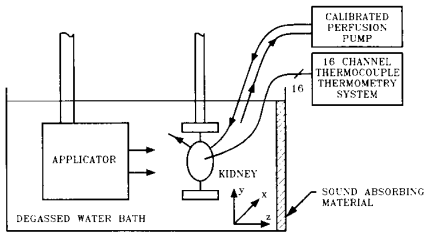

Fig. 1. Experimental setup.

temperatures, respectively; c_m and c_w are the specific heats of tissue and water, respectively; and ρ is the tissue density [17]. The effective perfusion can thus be calculated by measuring the time constant $\tau = \rho c_m / w_e c_w$ of the thermal washout curve.

The initial rate of temperature rise $(dT/dt)_0$, before appreciable heat loss due to conduction and perfusion occurs, was employed to estimate the ultrasonic intensity at the site of a thermocouple probe using the relationship [18]

$$I = \frac{\rho c_m}{2\alpha}\left(\frac{dT}{dt}\right)_0 \quad (3)$$

where α is the absorption coefficient in the tissue (Np $\cdot$ cm^{-1}).

C. Applicator

The phantom was insonated with a 1 MHz unfocused multielement ultrasound hyperthermia applicator [19], [20] at a distance of 7.6 cm from the applicator. The applicator contained 16 3.8 cm square individually controllable piezoelectric ceramic elements for an effective square aperture of 15.2 × 15.2 cm. Because of the relatively small dimensions of the porcine kidneys used in this study, approximately 7 × 3.5 × 2.5 cm (l × h × d), only two of the applicator elements were used. The relative and spatial average intensities produced by this applicator were previously measured using a hydrophone probe and a radiation force balance [19], [20]. The spatial variations in intensity have been shown to be less than 30% in the region of the field occupied by the phantom [21].

III. Results and Discussion

The absorption coefficient measured in four freshly excised and one alcohol fixed porcine kidneys, for both the cortex and medullary regions, are listed in Table I. The number of samples measured from each region for both types of kidney sample are indicated in the table. These measurements indicate that the absorption coefficient in the fixed kidney cortex is approximately equal to that in the freshly excised samples, whereas the absorption coefficient in the medullary tissue increased slightly with fixation. These results indicate that the absorption is essentially the same throughout the fixed kidney.

Fig. 2 shows a typical example of the measured temperature rise versus time when the phantom was perfused at a rate of 38.9 (±10%) kg $\cdot$ $m^{-3} \cdot s^{-1}$, for acoustical power outputs of 74 and 130 W per element, at a depth of 3 mm. The initial rates of temperature rise in these curves are 0.11 and 0.19°C s^{-1}, which correspond to intensities at the thermocouple sites of 5.1 and 8.8 (±15%) W $\cdot$ cm^{-2}, respectively. Because of the difficulty in precisely determining the positions of the thermocouples relative to the applicator, it was not possible to correlate these intensity measurements with those obtained with the hydrophone probe.

The temperature rise versus time response of the phantom with perfusion rates of 0, 13.2, and 19.8 (±10%) kg $\cdot$ $m^{-3} \cdot s^{-1}$, when insonified with 130 W of acoustical power per element is shown in Fig. 3. The intensity incident on the thermocouple was calculated to be 4.5 W $\cdot$ cm^{-2}. Using (2), W_e is calculated to be 4.5, 16.0, and 24.6 kg $\cdot$ $m^{-3} \cdot s^{-1}$ for these three curves. The differences between W_e and the average perfusion rate are most likely due to nonnegligible conduction effects and a local perfusion rate that may

TABLE I
ABSORPTION COEFFICIENT (Np cm^{-1}) IN ROH FIXED AND FRESH PORCINE KIDNEY AT 1 MHz

	Fixed		Fresh	
	Cortex	Medulla	Cortex	Medulla
# of samples	3	2	5	3
mean	0.044	0.042	0.041	0.033
SD	0.008	0.009	0.015	0.009

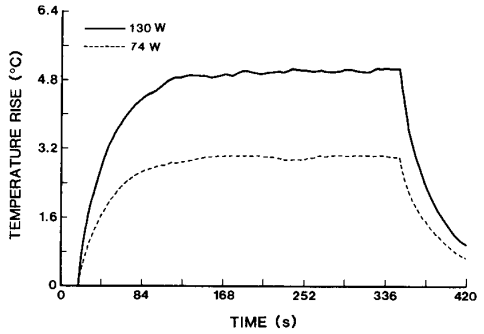

Fig. 2. Temperature rise versus time at a depth of 3 mm in the phantom, with acoustical power outputs of 74 and 130 W per element, and an average perfusion rate of 38.9 kg m^{-3} s^{-1}.

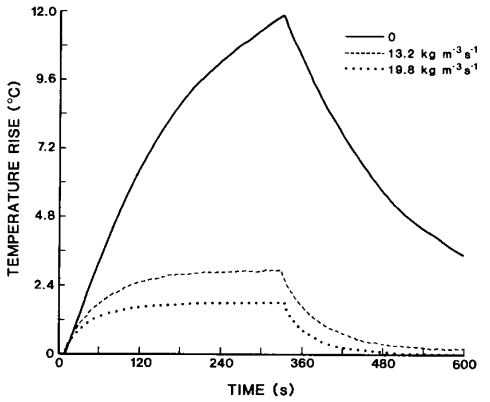

Fig. 3. Temperature rise versus time at a depth of 12 mm in the phantom, with a spatial average intensity of 4.5 W cm^{-2}.

differ from the average perfusion rate. Thus, while this simple thermal model allows the effective perfusion to be calculated, the values obtained should be used with caution when comparisons are made between locations in the phantom where effects of conduction and perfusion may vary.

Fig. 4 illustrates a steady-state temperature-rise distribution in an xz-plane slice through the cortex of the phantom both with and without perfusion. The increase in the heterogeneity of the temperature rises at depths greater than approximately $z = 10$ mm when the phantom is perfused is likely a result of variations in local perfusion. The variations in temperature rises near the front surface was likely due to heat conduction effects since those thermocouples closest to the surface were observed to consistently measure the lowest temperature rises.

Since the medulla has a somewhat irregular structure and is significantly smaller in size than the cortex (cortex was measured to comprise at least 85% of the weight of the pig kidney), it is difficult to accurately place thermocouples in it. However, once the thermocouples are in place, the thermocouples in the medulla can be distinguished from those in the cortex by their reduced response to changes in perfusion. Fig. 5 shows a profile of the temperature distribution in the z direction (depth) through the center of the perfused phantom. The temperature in the medulla ($z = 15$ mm) is markedly higher than the temperatures in the cortex. The cortex temperatures display the characteristic exponential decay with increasing depth due to attenuation losses. Similar profiles were observed for different applicator positions relative to the phantom which ruled out spatial variations in the applicator field as a contributing factor.

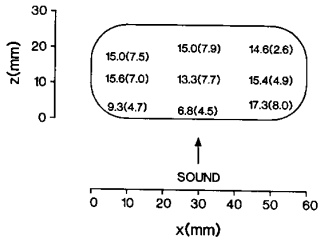

Fig. 4. Steady-state temperature rise versus position in an xz-plane slice through the cortex of the phantom, with an acoustical power output of 115 W per element and average perfusion rates of 0 and 19.8 kg m^{-3} s^{-1}. Temperatures for the perfused case are listed in parentheses.

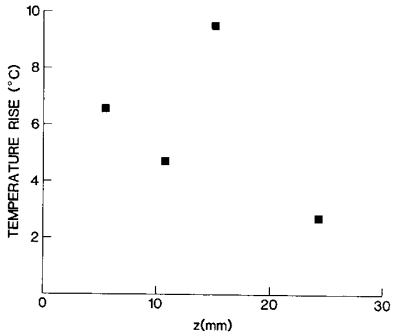

Fig. 5. Steady-state temperature rise versus depth in the phantom, with an acoustical power output of 100 W per element and an average perfusion rate of 7.3 kg m^{-3} s^{-1}.

VI. CONCLUSION

The fixed kidney phantom possesses thermal and absorptive properties that are comparable to those found in many human tissues. The fixation technique minimized the differences in the absorption coefficient between the cortex and medullary regions while maintaining the natural inhomogeneous perfusion. The phantom modeled the inhomogeneous perfusion found in tumors and could be perfused at rates commonly found in normal and tumor tissues.

Quantitative measurements of the incident intensity can easily and repeatedly be made in the phantom using thermocouple probes. The local perfusion in the phantom can also be estimated using temperature data from the probes and the simplified perfusion model. However, the size of the kidney limited the extent of the applicator's field that could be examined. Larger kidneys, such as the bovine kidney, would provide a larger target for the applicator which would be desirable for studying applicators with treatment fields greater than 25 cm^2.

The heterogeneity of the temperature distribution in the phantom suggests that variations in local perfusion and conduction together with spatial variations in the applicator field intensity greatly affects the ability to produce uniform temperature distributions in the phantom. Since the vasculature of the phantom is similar to that of many solid tumors, one can expect similar difficulties in uniformly heating well perfused solid tumors.

In light of the results obtained in this study, the perfused kidney phantom has the potential of serving as a simple, easy to use, and realistic model of perfused tumors for the evaluation of ultrasound hyperthermia applicators. However, further work is needed to determine the local flow variations in the phantom so that the discrepancy between the average perfusion rate and the corresponding effective rate can be addressed.

ACKNOWLEDGMENT

The authors wish to thank K. Carnes, J. Drewniak, S. Foster, J. McCarthy, and P. Neubauer for their technical assistance.

REFERENCES

[1] R. B. Roemer, W. Swindell, S. T. Clegg, and R. L. Kress, "Simulation of focused, scanned ultrasonic heating of deep-seated tumors: The effect of blood perfusion," *IEEE Trans. Sonics Ultrason.*, vol. SU-31, pp. 457-466, 1984.

[2] K. B. Ocheltree and L. A. Frizzell, "Determination of power deposition patterns for localized hyperthermia: A steady state analysis," *Int. J. Hyperthermia*, vol. 3, pp. 269-279, 1987.

[3] ——, "Determination of power deposition patterns for localized hyperthermia: A transient analysis," *Int. J. Hyperthermia*, vol. 4, pp. 281-296, 1988.

[4] R. P. Roemer, "Ultrasound phantoms/animal experiments," in *Physics and Technology of Hyperthermia*, S. B. Field and C. Franconi, Eds. Dordrecht: Martinus Nijhoff, 1987, pp. 403-413.

[5] J. W. Baish, K. R. Foster, and P. S. Ayyaswamy, "Perfused phantom models of microwave irradiated tissue," *J. Biomechan. Eng.*, vol. 108, pp. 239-245, 1986.

[6] T. S. Sandhu, "Thermal dosimetry system with blood flow simulation," *NCI Monograph*, vol. 61, pp. 513-515, 1982.

[7] K. Hynynen, R. Roemer, D. Anhalt, C. Johnson, Z. X. Xu, W. Swindell, and T. Cetas, "A scanned, focused, multiple transducer ultrasonic system for localized hyperthermia treatments," *Int. J. Hyperthermia*, vol. 3, no. 1, pp. 21-35, 1987.

[8] P. R. Stauffer, S. A. Suen, T. Satoh, J. R. Fike, and P. K. Sneed, "Validity of an in vivo tissue model for hyperthermia dosimetry," in *Proc. IEEE/Ninth Ann. Conf. Eng. Med. Biol. Soc.*, 1987, pp. 997-999.

[9] B. Endrich, H. A. Reinhold, J. F. Gross, and M. Intaglietta, "Tissue perfusion inhomogeneity during early tumor growth in rats," *J. Nat. Cancer Inst.*, vol. 62, pp. 387-395, 1979.

[10] K. R. Holmes, W. Ryan, P. Weinstein, and M. M. Chen, "A fixation technique for organs to be used as perfused tissue phantoms in bioheat transfer studies," in *1984 Advances in Bioengineering*, by R. L. Spiker, Ed. New York: Amer. Soc. Mech. Eng., 1984, pp. 9-10.

[11] K. R. Holmes, W. Ryan, and M. M. Chen, "Thermal conductivity and H_2O content in the rabbit kidney cortex and medulla," *J. Therm. Biol.*, vol. 8, pp. 311-313, 1983.

[12] K. Diem and C. Lentner, *Geigy Scientific Tables*. New York: Geigy Pharmaceuticals/Ardsley, 1974.

[13] T. E. Cooper and G. J. Trezek, "Correlation of the thermal properties of some human tissue with water content," *Aerosp. Med.*, vol. 42, pp. 24-27, 1971.

[14] R. K. Jain and K. Ward-Hartley, "Tumor blood flow—Characterization, modifications, and role in hyperthermia," *IEEE Trans. Sonics Ultrason.*, vol. SU-31, pp. 504-525, 1984.

[15] W. J. Fry and R. B. Fry, "Determination of absolute sound levels and acoustic absorption coefficients by thermocouple probes—Theory," *J. Acoust. Soc. Amer.*, vol. 26, pp. 294-310, 1954.

[16] ——, "Determination of absolute sound levels and acoustic absorption coefficients by thermocouple probes—Experiment," *J. Acoust. Soc. Amer.*, vol. 26, pp. 311-317, 1954.

[17] A. W. Guy, J. F. Lehmann, and J. R. Stonebridge, "Therapeutic applications of electromagnetic power," *Proc. IEEE*, vol. 62, pp. 55-75, 1974.

[18] W. L. Nyborg, "Heat generation by ultrasound in a relaxing medium," *J. Acoust. Soc. Amer.*, vol. 70, pp. 310-312, 1981.

[19] H. R. Underwood, E. C. Burdette, K. B. Ocheltree, and R. L. Magin, "A multielement ultrasonic hyperthermia applicator with independent element control," *Int. J. Hyperthermia*, vol. 3, no. 3, pp. 257-267, 1987.

[20] P. J. Benkeser, L. A. Frizzell, S. A. Goss, and C. A. Cain, "Analysis of a multielement ultrasound hyperthermia applicator," *IEEE Trans. Ultrason. Ferroelect. Freq. Contr.*, vol. 36, no. 4, pp. 319-325, 1989.

Multichannel Physiological Monitor Plus Simultaneous Full-Duplex Speech Channel Using a Dial-Up Telephone Line

M. REZAZADEH AND N. E. EVANS

***Abstract*—Because of bandwidth limitations, the Public Switched Telephone Network (PSTN) cannot normally accommodate simultaneous multichannel physiological signaling with speech. This communication describes work carried out to build a physiological monitoring system which can transmit up to six low-frequency data channels in the presence of a full-duplex speech channel using one telephone line.**

INTRODUCTION

Electrocardiograms were transmitted over telephone lines by Einthoven as early as 1905 [1]. More recent work has resulted in multichannel systems using frequency multiplexed FM across the whole telephone bandwidth [2].

Multichannel physiological data transmission is important because

1) It allows the transmission of certain multilead signals which must be received simultaneously to be of any value; the transmission of vector cardiograms is an example. Also, as has been shown in the case of epileptic patients, it is sometimes necessary to monitor the ECG together with the EEG since some patients show irregularities in the background recording before the time of an epileptic attack [3], [4].

2) Parallel signalling speeds up the transmission of multilead data.

Simultaneous speech and data communication can be useful in telephone defibrillation and also for patients who need to self-administer drugs [5].

THE TELEPHONE SYSTEM AND SPEECH SIGNALS

The bandwidth of a typical telephone line is about 3.1 kHz, extending from 300 to 3400 Hz. In order to accommodate the six channels of physiological data, the speech channel in our system is sharply bandlimited at about 2.5 kHz using a seventh-order elliptic low-pass filter. The remaining telephone-line spectrum then becomes available for data transmission. Such severe filtering of the speech signal is perfectly justifiable in communications terms. Syllabic articulation tests have shown that there is not a great change in percentage sound articulation between a 2500 and 3500 Hz cutoff frequency [6].

The seventh-order low-pass active elliptic filter used to bandlimit the speech on the telephone line was designed around three

Manuscript received January 11, 1989; revised July 11, 1989. This work was supported by the Northern Ireland Bioengineering Center.

M. Rezazadeh is with the Northern Ireland Bioengineering Center, University of Ulster, Newtownabbey, Co. Antrim, BT37 0QB, Northern Ireland.

N. E. Evans is with the Department of Electrical and Electronic Engineering, University of Ulster, Newtownabbey, Co. Antrim, BT37, 0QB, Northern Ireland.

IEEE Log Number 8933603.